The Operational Space Formulation in the Analysis, Design, and Control of Robot Manipulators

Oussama Khatib

Artificial Intelligence Laboratory
Computer Science Department, Stanford University
Stanford, California, USA

Manipulator action is primarily characterized by the end-effector motion and exerted forces. The description of the dynamic behavior of this basic component in the manipulator mechanism has been the impetus for the work in the operational space formulation. The end-effector equations of motion developed in this formulation are the fundamental tool for the analysis, design and control of manipulators with respect to their end-effector performance. Using this end-effector dynamic model, we investigate the dynamic characterization of manipulators and formalize the problem of dynamic optimization in manipulator design. In manipulator control, we present a unified approach to real-time dynamic control and active force control. A generalized position and force specification matrix for task description is used in the formulation of the unified command vector of operational forces. We also present the extension of this approach to redundant manipulator mechanisms, and discuss kinematic singularity problems. A two-level control system architecture has been designed to increase the system's real-time performance

1. Introduction

Research in dynamics of robot mechanisms has largely focused on developing the equations of joint motions. These joint space dynamic models have been the basis for various approaches to dynamic control of manipulators. However, task specification for motion and applied forces, dynamics, and force sensing feedback, are closely linked to the end-effector. The dynamic behaviour of the end-effector is one of the most significant characteristics in evaluating the performance of robot manipulator systems. The issue of end-effector motion control has been investigated and algorithms resolving end-effector accelerations have been developed [Takase 1977; Khatib, Llibre, and Mampey 1978; Hewit and Padovan 1978; Renaud, and Zabala-Iturralde 1979; Luh, Walker, and Paul 1980].

Precise control of applied end-effector forces is crucial to accomplishing advanced robot assembly tasks. An extensive research effort has been devoted to the study of manipulator force control. Recently, Whitney [Whitney 1985] presented a detailed review of the work in force control. Accommodation [Whitney 1977], joint compliance [Paul and Shimano 1976], active compliance [Salisbury 1980], passive compliance, and hybrid position/force control [Craig and Raibert 1979] are among the various methods that have been proposed. Active force control has been generally based on kinematic considerations, and has been treated within the framework of joint space control systems. The very approach of joint space control is ill-suited to the integration of active force control, and we will show how this problem can be addressed naturally in the framework of operational space control systems.

The *operational space formulation* [Khatib 1980, Khatib 1983], which establishes the end-effector equations of motion, has its roots in the work on end-effector motion control [Khatib, Llibre, and Mampey 1978] and obstacle avoidance [Khatib and Le Maitre 1978]. In this paper, we will review the fundamentals of this formulation, present a unified approach for the control of motion and applied forces, and describe the two-level control system architecture that has been designed to increase the system's real-time capabilities.

Redundancy in manipulator systems has been used to achieve goals such as the minimization of a quadratic criterion [Whitney 1969, Renaud 1975], the avoidance of joint limits [Liegois 1977, Four- nier 1980], improvement of singularity characteristics and the avoidance of obstacles [Hanafusa, Yoshikawa, and Nakamura 1981, Hollerbach 1984, Luh and Gu 1985], and the minimization of actuator joint forces [Hollerbach and Suh 1985]. In this paper, we will present the extension of the operational space formulation to redundant mechanisms and consider their stability. We will also discuss the problems arising at kinematic singularities.

Research on the kinematics of articulated mechanisms has developed means for the analysis of workspace characteristics [Roth 1976, Shimano 1978], and the evaluation of kinematic performance [Fournier1980, Paul and Stevenson 1983]. Yoshikawa [Yoshikawa 1983] has proposed a *measure of manipulability* for the evaluation of manipulator kinematic performance. Kinematic and static force characteristics also have been investigated [Asada and Cro Granito 1985].

Dynamic characterization is an essential consideration in the analysis, design, and control of these nonlinear, coupled, and multi-body mechanisms. Asada proposed the generalized inertia ellipsoid [Asada 1983] as a tool for the characterization of manipulator dynamics. The *measure of manipulability* has recently been extended to a *measure of dynamic manipulability* [Yoshikawa 1985].

The dynamic performance is characterized [Khatib and Burdick 1985] by the magnitude of the isotropic acceleration that is available at the end-effector in a given configuration and at a given velocity. The dynamic optimization is achieved by maximizing this criterion throughout the workspace.

2. Operational Space Formulation

Let $x_1, x_2, \ldots, x_m$ be a set of m *configuration parameters* of the end-effector, describing its position and orientation in a frame of reference $\mathcal{R}_0$. An *operational coordinate system* is a set x of m_0 *independent* end-effector configuration parameters.

Robotics Research 3, Cambridge: MIT Press, 1986

Let us first consider the case of non-redundant manipulators and use a set of independent parameters, *i.e.* operational coordinates, to represent the end-effector configuration ($n = m_0$). For a non-redundant manipulator, the independent parameters $x_1, x_2, \ldots, x_{m_0}$ form a complete set of configuration parameters in a domain of the operational space [Khatib 1980] and thus constitute a system of generalized coordinates. The end-effector equations of motion in operational space can be written as [Khatib 1980, Khatib 1983]

$$\Lambda(\mathbf{x})\ddot{\mathbf{x}} + \mu(\mathbf{x},\dot{\mathbf{x}}) + \mathbf{p}(\mathbf{x}) = \mathbf{F}; \tag{1}$$

where $\Lambda(\mathbf{x})$ designates the kinetic energy matrix, and $\mu(\mathbf{x},\dot{\mathbf{x}})$ represents the vector of end-effector centrifugal and Coriolis forces. $\mathbf{p}(\mathbf{x})$ and $\mathbf{F}$ are respectively the gravity and the generalized operational force vectors. The i^{th} component of $\mu(\mathbf{x},\dot{\mathbf{x}})$ can be written as

$$\mu_i(\mathbf{x},\dot{\mathbf{x}}) = \dot{\mathbf{x}}^T \Pi_i(\mathbf{x})\dot{\mathbf{x}}; \tag{2}$$

where the components of the $m_0 \times m_0$ matrix $\Pi_i(\mathbf{x})$ are the Christoffel symbols $\pi_{i,jk}$ given as a function of the partial derivatives of $\Lambda(\mathbf{x})$ *w.r.t.* the generalized coordinates $\mathbf{x}$ by:

$$\pi_{i,jk} = \frac{1}{2}\left(\frac{\partial \lambda_{ij}}{\partial x_k} + \frac{\partial \lambda_{ik}}{\partial x_j} - \frac{\partial \lambda_{jk}}{\partial x_i}\right). \tag{3}$$

With respect to a system of n joint coordinates $\mathbf{q}$, the equations of motion in joint space can be written in the form:

$$A(\mathbf{q})\ddot{\mathbf{q}} + \mathbf{b}(\mathbf{q},\dot{\mathbf{q}}) + \mathbf{g}(\mathbf{q}) = \Gamma; \tag{4}$$

where $\mathbf{b}(\mathbf{q},\dot{\mathbf{q}})$, $\mathbf{g}(\mathbf{q})$, and Γ, represent the Coriolis and centrifugal, gravity, and generalized forces in joint space; and $A(\mathbf{q})$ is the $n \times n$ joint space kinetic energy matrix, which is related to $\Lambda(\mathbf{x})$ by:

$$A(\mathbf{q}) = J^T(\mathbf{q})\Lambda(\mathbf{x})J(\mathbf{q}). \tag{5}$$

3. End-Effector Motion Control

The control of manipulators in operational space is based on the selection of $\mathbf{F}$ as a command vector. In order to produce this command, specific forces Γ must be applied with joint-based actuators. With $\mathbf{q}$ representing the vector of n joint coordinates and $J(\mathbf{q})$ the Jacobian matrix, the relationship between $\mathbf{F}$ and the generalized joint forces Γ is given by:

$$\Gamma = J^T(\mathbf{q})\,\mathbf{F}. \tag{6}$$

While in motion, a manipulator end-effector is subject to the inertial coupling, centrifugal, and Coriolis forces. These non-linearities can be compensated for by dynamic decoupling in operational space using the end-effector equations of motion (1). The operational command vector for the end-effector dynamic decoupling and motion control is

$$\mathbf{F} = \mathbf{F}_m + \mathbf{F}_{ccg}; \tag{7}$$

with

$$\begin{aligned} \mathbf{F}_m &= \Lambda(\mathbf{x})\mathbf{F}^*_m; \\ \mathbf{F}_{ccg} &= \mu(\mathbf{x},\dot{\mathbf{x}}) + \mathbf{p}(\mathbf{x}); \end{aligned} \tag{8}$$

where $\mathbf{F}^*_m$ is the command vector of the decoupled end-effector. The end-effector becomes equivalent to a *single unit mass* moving in the m_0-dimensional space. Using equation (6), the joint forces corresponding to the operational command vector $\mathbf{F}$ in (7) can be written as

$$\Gamma = J^T(\mathbf{q})\Lambda(\mathbf{q})\mathbf{F}^*_m + \tilde{\mathbf{b}}(\mathbf{q},\dot{\mathbf{q}}) + \mathbf{g}(\mathbf{q}); \tag{9}$$

where $\tilde{\mathbf{b}}(\mathbf{q},\dot{\mathbf{q}})$ is the vector of joint forces under the mapping into joint space of the end-effector Coriolis and centrifugal force vector $\mu(\mathbf{x},\dot{\mathbf{x}})$. In order to simplify the notation, the symbol Λ has also been used here to designate the kinetic energy matrix when expressed as a function of the joint coordinate vector $\mathbf{q}$. $\tilde{\mathbf{b}}(\mathbf{q},\dot{\mathbf{q}})$ is distinct from the vector of centrifugal and Coriolis forces $\mathbf{b}(\mathbf{q},\dot{\mathbf{q}})$ that arise when viewing the manipulator motion in joint space. These vectors are related by:

$$\tilde{\mathbf{b}}(\mathbf{q},\dot{\mathbf{q}}) = \mathbf{b}(\mathbf{q},\dot{\mathbf{q}}) - J^T(\mathbf{q})\Lambda(\mathbf{q})\mathbf{h}(\mathbf{q},\dot{\mathbf{q}}); \tag{10}$$

where

$$\mathbf{h}(\mathbf{q},\dot{\mathbf{q}}) = \dot{J}(\mathbf{q})\dot{\mathbf{q}}. \tag{11}$$

A useful form of $\tilde{\mathbf{b}}(\mathbf{q},\dot{\mathbf{q}})$ for real-time control and dynamic analysis is

$$\tilde{\mathbf{b}}(\mathbf{q},\dot{\mathbf{q}}) = \tilde{B}(\mathbf{q})[\dot{\mathbf{q}}\dot{\mathbf{q}}] + \tilde{C}(\mathbf{q})[\dot{\mathbf{q}}^2]; \tag{12}$$

where $\tilde{B}(\mathbf{q})$ and $\tilde{C}(\mathbf{q})$ are the $n \times n(n-1)/2$ and $n \times n$ matrices of the joint forces under the mapping into joint space of the end-effector Coriolis and centrifugal forces. $[\dot{\mathbf{q}}\dot{\mathbf{q}}]$ and $[\dot{\mathbf{q}}^2]$ are the symbolic notations for the $n(n-1)/2 \times 1$ and $n \times 1$ column matrices

$$\begin{aligned} [\dot{\mathbf{q}}\dot{\mathbf{q}}] &= [\dot{q}_1\dot{q}_2 \;\; \dot{q}_1\dot{q}_3 \ldots \dot{q}_{n-1}\dot{q}_n]^T; \\ [\dot{\mathbf{q}}^2] &= [\dot{q}_1^2 \;\; \dot{q}_2^2 \ldots \dot{q}_n^2]^T. \end{aligned} \tag{13}$$

With the relation (12), the dynamic decoupling of the end-effector can be obtained using the configuration dependent dynamic coefficients $\Lambda(\mathbf{q})$, $\tilde{B}(\mathbf{q})$, $\tilde{C}(\mathbf{q})$ and $\mathbf{g}(\mathbf{q})$. By isolating these coefficients, end-effector dynamic decoupling and control can be achieved in a two-level control system architecture. The real-time computation of these coefficients can then be paced by the rate of configuration changes, which is much lower than that of the mechanism dynamics. Furthermore, the rate of computation of the end-effector position can be reduced by integrating an operational position estimator into the control system. Finally, the control system has the following architecture (see Figure 1):

- A low rate *parameter evaluation level*: updating the end-effector dynamic coefficents, the Jacobian matrix, and the geometric model.
- A high rate *servo control level*: computing the command vector using the estimator and the updated dynamic coefficients.

4. Active Force Control

Tasks are generally described in terms of end-effector motion and applied forces and torques. Let $\mathbf{f}_d$ and τ_d be the vectors, in the frame of reference $\mathcal{R}_0(O, \mathbf{x}_0, \mathbf{y}_0, \mathbf{z}_0)$, of forces and torques that are to be applied by the end-effector. The position of the end-effector can be controlled for motions specified in the subspace orthogonal to f_d. Let $\mathcal{R}_f(O, \mathbf{x}_f, \mathbf{y}_f, \mathbf{z}_f)$ be a frame of reference resulting from $\mathcal{R}_0$ by a rotation transformation S_f such that $\mathbf{z}_f$ is in alignment with f_d. In $\mathcal{R}_f$, the largest subspace of position control is spanned by $\{\mathbf{x}_f, \mathbf{y}_f\}$. With a task specified in terms of end-effector position control in $\{\mathbf{x}_f, \mathbf{y}_f\}$ and force control following $\mathbf{z}_f$, we associate the task specification matrix

$$\Sigma_f = \begin{pmatrix} 1 & 0 & 0 \\ 0 & 1 & 0 \\ 0 & 0 & 0 \end{pmatrix}. \tag{14}$$

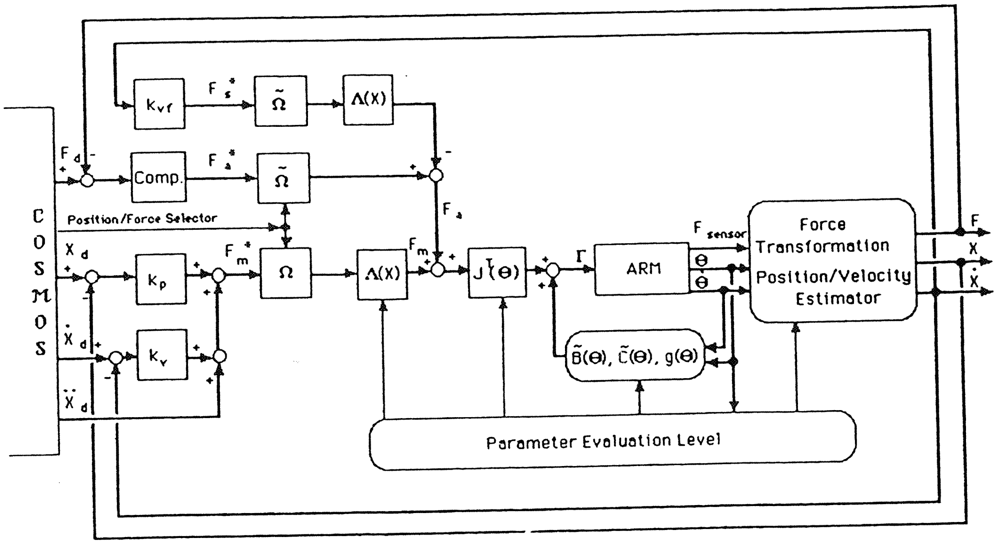

Figure 1. *Operational Space Control System Architecture*

If, in addition, a free motion (zero controlled force) in a direction of the subspace orthogonal to $\mathbf{f}_d$ is specified, the frame of reference $\mathcal{R}_f$ can be selected in order to align its $\mathbf{y}_f$ axis with that direction, and the corresponding diagonal element in Σ_f will then be zero. For tasks that specify free motions in the plane orthogonal to $\mathbf{f}$, Σ_f becomes the 3×3 zero matrix.

Similarly, let $\mathcal{R}_\tau(\mathcal{O}, \mathbf{x}_\tau, \mathbf{y}_\tau, \mathbf{z}_\tau)$ be a frame of reference obtained from $\mathcal{R}_0(\mathcal{O}, \mathbf{x}_0, \mathbf{y}_0, \mathbf{z}_0)$ by a rotation S_τ that brings $\mathbf{z}_\tau$ into alignment with the task torque vector τ_d. In $\mathcal{R}_\tau$, the subspace of end-effector rotations is spanned by $\{\mathbf{x}_\tau, \mathbf{y}_\tau\}$. The matrix Σ_τ of task specification associated with this task of rotations and applied torques described in $\mathcal{R}_\tau$ is similar to Σ_f. Finally, for general tasks of end-effector position (position and orientation) and applied forces (forces and torques) described in the frame of reference $\mathcal{R}_0$ we define *the generalized position and force specification matrix*

$$\Omega = \begin{pmatrix} S_f^T \Sigma_f S_f & 0 \\ 0 & S_\tau^T \Sigma_\tau S_\tau \end{pmatrix}. \tag{15}$$

Using Ω, the unified operational command vector for end-effector dynamic decoupling, motion, and active force control can be written as

$$\mathbf{F} = \mathbf{F}_m + \mathbf{F}_a + \mathbf{F}_{ccg}; \tag{16}$$

where $\mathbf{F}_m$, $\mathbf{F}_a$ are the operational command vectors of motion and active force control, given by:

$$\begin{aligned} \mathbf{F}_m &= \Lambda(\mathbf{q})\Omega\mathbf{F}^*_m \\ \mathbf{F}_a &= \tilde{\Omega}\mathbf{F}^*_a + \Lambda(\mathbf{q})\tilde{\Omega}\mathbf{F}^*_s; \end{aligned} \tag{17}$$

where $\mathbf{F}^*_s$ represents the vector of end-effector velocity damping that acts in the direction of f_d and about the axis of τ_d. The matrix $\tilde{\Omega}$ is given by

$$\tilde{\Omega} = \begin{pmatrix} S_f^T \overline{\Sigma}_f S_f & 0 \\ 0 & S_\tau^T \overline{\Sigma}_\tau S_\tau \end{pmatrix}; \tag{18}$$

where

$$\begin{aligned} \overline{\Sigma}_f &= I - \Sigma_f; \\ \overline{\Sigma}_\tau &= I - \Sigma_\tau. \end{aligned} \tag{19}$$

The joint force vector corresponding to $\mathbf{F}$ in (16), is

$$\Gamma = J^T(\mathbf{q})[\Lambda(\mathbf{q})(\Omega\mathbf{F}^*_m + \tilde{\Omega}\mathbf{F}^*_s) + \tilde{\Omega}\mathbf{F}^*_a] + \tilde{\mathbf{b}}(\mathbf{q}, \dot{\mathbf{q}}) + \mathbf{g}(\mathbf{q}). \tag{20}$$

I designates the 3×3 identity matrix. The control system architecture is shown in Figure 1, where k_{vf} denotes the velocity gain in $\mathbf{F}^*_s$. A more detailed description of this control system is presented in [Khatib and Burdick 1986].

This approach has been implemented in an experimental manipulator programming system COSMOS (Control in Operational Space of a Manipulator-with-Obstacles System). Using a PUMA 560 and wrist and finger sensing, demonstrations of real-time end-effector motion and active force control operations have been performed. These include contact, slide, insertion, and compliance operations [Khatib, Burdick, and Armstrong 1985], as well as real-time collision avoidance with links and moving obstacles [Khatib 1985]. In the current multiprocessor implementation (PDP 11/45 and PDP 11/60), the rate of the servo control level is 225 Hz while the coefficient evaluation level runs at 100 Hz.

5. Redundant Manipulators

For a redundant manipulator, the configuration of the entire system cannot be specified by a set of parameters that describes only the end-effector position and orientation. An independent set of end-effector configuration parameters, therefore, does not constitute a generalized coordinate system for a redundant manipulator, and the dynamic behavior of the entire redundant system cannot be represented by a dynamic model in coordinates only of the end-effector configuration. The dynamic behavior of the *end-effector* itself, nevertheless, can still be described in its configuration coordinates, and its equations of motion in operational space can still be established. While these equations of motion can be used to achieve control of the end-effector motions and active forces, further analysis for the global stabilization of the redundant mechanism is required, and must be based on the manipulator joint space dynamic model.

Using the dynamic model (4) and the relation

$$\ddot{\mathbf{x}} = J(\mathbf{q})\ddot{\mathbf{q}} + \mathbf{h}(\mathbf{q}, \dot{\mathbf{q}}); \tag{21}$$

we established [Khatib 1980] the following equations of motion for a redundant manipulator system

$$\Lambda_r(\mathbf{x})\ddot{\mathbf{x}} + \mu_r(\mathbf{x},\dot{\mathbf{x}}) + \mathbf{p}_r(\mathbf{x}) = \mathbf{F}; \tag{22}$$

where

$$\begin{aligned}\Lambda_r(\mathbf{q}) &= [J(\mathbf{q})A^{-1}(\mathbf{q})J^T(\mathbf{q})]^{-1};\\ \mu_r(\mathbf{q},\dot{\mathbf{q}}) &= \bar{J}^T(\mathbf{q})\mathbf{b}(\mathbf{q},\dot{\mathbf{q}}) - \Lambda_r(\mathbf{q})\mathbf{h}(\mathbf{q},\dot{\mathbf{q}});\\ \mathbf{p}_r(\mathbf{q}) &= \bar{J}^T(\mathbf{q})\mathbf{g}(\mathbf{q});\end{aligned} \tag{23}$$

with

$$\bar{J}(\mathbf{q}) = A^{-1}(\mathbf{q})J^T(\mathbf{q})\Lambda_r(\mathbf{q}). \tag{24}$$

$\bar{J}(\mathbf{q})$ is actually a pseudo-inverse of the Jacobian matrix corresponding to the solution that minimizes the manipulator's kinetic energy. Dynamic decoupling and control of the end-effector can then be obtained using a control system similar to that of (20)

$$\Gamma = J^T(\mathbf{q})[\Lambda_r(\mathbf{q})(\Omega\mathbf{F}^*_m + \tilde{\Omega}\mathbf{F}^*_s) + \tilde{\Omega}\mathbf{F}^*_a] + \tilde{\mathbf{b}}_r(\mathbf{q},\dot{\mathbf{q}}) + \mathbf{g}(\mathbf{q}); \tag{25}$$

where $\tilde{\mathbf{b}}_r(\mathbf{q},\dot{\mathbf{q}})$ is the vector of joint forces under the mapping into joint space of the end-effector Coriolis and centrifugal force vector $\mu_r(\mathbf{x},\dot{\mathbf{x}})$. Like $\tilde{\mathbf{b}}(\mathbf{q},\dot{\mathbf{q}})$, the vector $\tilde{\mathbf{b}}_r(\mathbf{q},\dot{\mathbf{q}})$ can be expressed as

$$\tilde{\mathbf{b}}_r(\mathbf{q},\dot{\mathbf{q}}) = \tilde{B}_r(\mathbf{q})[\dot{\mathbf{q}}\dot{\mathbf{q}}] + \tilde{C}_r(\mathbf{q})[\dot{\mathbf{q}}^2]. \tag{26}$$

Under the command vector(24), the manipulator is subject to the dissipative forces Γ_{dis} due to the $\dot{\mathbf{x}}$ term in $\mathbf{F}^*_m$

$$\Gamma_{dis} = D(\mathbf{q})\dot{\mathbf{q}}; \tag{27}$$

with

$$D(\mathbf{q}) = -k_v J^T(\mathbf{q})\Lambda_r(\mathbf{q})J(\mathbf{q}). \tag{28}$$

$D(\mathbf{q})$ is an $n \times n$ negative semi-definite matrix of rank m_0. Although the stability condition [Mingori 1970]

$$\dot{\mathbf{q}}^T D(\mathbf{q})\dot{\mathbf{q}} \le 0; \tag{29}$$

of the articulated mechanical system (4) under the previous command is satisfied, this redundant mechanism can still describe movements that are solutions of the equation [Rumiantsev 1970]

$$\dot{\mathbf{q}}^T D(\mathbf{q})\dot{\mathbf{q}} = 0. \tag{30}$$

Asymptotic stabilization of the system can be achieved by the addition of dissipative forces proportional to $\dot{\mathbf{q}}$ [Khatib 1980]. These forces can be selected from the null space of the Jacobian matrix. This precludes any effect of the additional forces on the end-effector and maintains its dynamic decoupling. Using the joint space dynamic model (4), this corresponds to applying the additional stabilizing joint forces

$$\Gamma_s = -k_{vq}A(\mathbf{q})[I - \bar{J}(\mathbf{q})J(\mathbf{q})]\dot{\mathbf{q}}. \tag{31}$$

By grouping the term $k_{vq}A(\mathbf{q})\bar{J}(\mathbf{q})J(\mathbf{q})]\dot{\mathbf{q}}$ of (31) with the dissippative forces in $\mathbf{F}^*_m$, the joint force command vector can be written in the form

$$\begin{aligned}\Gamma = {} & J^T(\mathbf{q})[\Lambda_r(\mathbf{q})(\Omega\mathbf{F}^*_m + \tilde{\Omega}\mathbf{F}^*_s) + \tilde{\Omega}\mathbf{F}^*_a]\\ & -k_{vq}A(\mathbf{q})\dot{\mathbf{q}} + \tilde{\mathbf{b}}_r(\mathbf{q},\dot{\mathbf{q}}) + \mathbf{g}(\mathbf{q});\end{aligned} \tag{32}$$

where in the case of a task with specified motion, $\mathbf{F}^*_m$, is given by

$$\mathbf{F}^*_m = \ddot{\mathbf{x}}_d - k_p(\mathbf{x} - \mathbf{x}_d) - k_v(\dot{\mathbf{x}} - \dot{\mathbf{x}}_d) + k_{vq}\dot{\mathbf{x}}; \tag{33}$$

where $\mathbf{x}_d$, $\dot{\mathbf{x}}_d$ and $\ddot{\mathbf{x}}_d$ are respectively the desired position, velocity and acceleration of the end-effector, and k_p and k_v are the position and velocity gains. The matrix $D(\mathbf{q})$ corresponding to the new expression for the dissipative joint forces Γ_{dis} in the command vector (32) becomes

$$D(\mathbf{q}) = -[(k_v - k_{vq})J^T(\mathbf{q})\Lambda_r(\mathbf{q})J(\mathbf{q}) + k_{vq}A(\mathbf{q})]. \tag{34}$$

Now, $D(\mathbf{q})$ is a negative definite matrix and the closed loop system is asymptotically stable.

6. Singular Configurations

A *singular configuration* is a configuration $\mathbf{q}$ at which the end-effector loses the ability to move along or rotate about some direction of the Cartesian space. In such a configuration, the manipulator's mobility locally decreases. To each singular configuration there corresponds a singular "direction" in operational space. It is for that direction, in fact, that the end-effector presents infinite inertial mass for displacements or infinite inertia for rotations. Its movements remain free, however, in the subspace orthogonal to this direction. The basic concept in our approach to the problem of kinematic singularities is:

At a singular configuration, the manipulator can be treated as a mechanism that is redundant with respect to the motion of the end-effector in the subspace of operational space which is orthogonal to its singular direction.

The equations of motion of the end-effector in that subspace are similar to those of a redundant mechanism. In addition, joint forces from the Jacobian null space can be used to select the desired configuration of the manipulator from among the various ones it can take for a given motion of the end-effector.

7. End-Effector Dynamic Performance

When evaluating the dynamic performance of a manipulator, we are primarily concerned with the dynamic characteristics of the end-effector in the manipulator workspace. In particular, the end-effector acceleration performance is one of the most important characteristics in the evaluation of the manipulator dynamic behavior.

Let us examine the operational command vector $\mathbf{F}$ in (7). Only a fraction of these operational forces, specifically $\mathbf{F}^*_m$ the input of the decoupled end-effector, contribute to the end-effector acceleration. The performance of end-effector motion and force control are strongly dependent on the magnitudes of the command vectors $\mathbf{F}^*_m$ and $\mathbf{F}_a$ that are available in a given configuration and at a given velocity.

Desired end-effector motions and applied forces are specified in orthogonal subspaces of the operational space. The evaluation of end-effector uniformity and isotropicity characteristics requires a complete analysis of its behavior in motion and applied forces throughout the workspace. Thus, for the most general performance analysis of end-effector motion (*respectively*, applied forces), the subspace associated with motion (*resp.* applied forces) will be expanded to the entire operational space.

For the performance analysis of end-effector applied forces, only static forces are significant, and the relevant relationship can be established with respect to the desired applied forces $\mathbf{F}_d$ as

$$\mathbf{F}_d = J^{-T}(\mathbf{q})[\Gamma - \mathbf{g}(\mathbf{q})]. \tag{35}$$

For end-effector motion performance, the relationship between

$\mathbf{F}^*_m$ and joint forces can be obtained from (9) as

$$\mathbf{F}^*_m = E(\mathbf{q})[\Gamma - \tilde{\mathbf{b}}(\mathbf{q}, \dot{\mathbf{q}}) - \mathbf{g}(\mathbf{q})]; \quad (36)$$

where

$$E(\mathbf{q}) = [J^T(\mathbf{q})\Lambda(\mathbf{q})]^{-1}. \quad (37)$$

Since $\mathbf{F}^*_m$ is the input of the decoupled unit mass end-effector, the matrix $E(\mathbf{q})$ also establishes the relationship between joint forces and end-effector accelerations

$$\ddot{\mathbf{x}} = E(\mathbf{q})[\Gamma - \tilde{\mathbf{b}}(\mathbf{q}, \dot{\mathbf{q}}) - \mathbf{g}(\mathbf{q})]. \quad (38)$$

Using equation (5), $E(\mathbf{q})$ can be written as $J(\mathbf{q})A^{-1}(\mathbf{q})$. Further expansion of (38) yields

$$\ddot{\mathbf{x}} - \mathbf{h}(\mathbf{q}, \dot{\mathbf{q}}) = E(\mathbf{q})[\Gamma - \mathbf{b}(\mathbf{q}, \dot{\mathbf{q}}) - \mathbf{g}(\mathbf{q})]; \quad (39)$$

which can also be obtained from the joint space dynamic model (4) and equation (21). The *measure of dynamic manipulability* [Yoshikawa 1985] has been based on the relation(39). This equation relates the manipulator generalized forces Γ corrected for gravity $\mathbf{g}(\mathbf{q})$ and the joint space centrifugal and Coriolis forces $\mathbf{b}(\mathbf{q}, \dot{\mathbf{q}})$ to a "pseudo" acceleration vector. This vector consists of the end-effector acceleration corrected for the vector $\mathbf{h}(\mathbf{q}, \dot{\mathbf{q}})$ of (11), which has been interpreted as a virtual acceleration. However, this vector is part of the joint force vector $\tilde{\mathbf{b}}(\mathbf{q}, \dot{\mathbf{q}})$ corresponding to the end-effector centrifugal and Coriolis force vector $\mu(\mathbf{x}, \dot{\mathbf{x}})$.

The initial definition of the measure of dynamic manipulability is based solely on the matrix $E(\mathbf{q})$ and is therefore not affected by the particular relationship used between joint forces and accelerations. Nevertheless, the extension of this measure to account for actuators and nonlinear forces yields an evaluation with respect to the pseudo acceleration vector, rather than to the actual acceleration of the end-effector.

Equations (35) and (36) establish the basic relationships for the evaluation of end-effector performance in motion and applied forces. In the following sections, we will focus on manipulator dynamic optimization with respect to end-effector motion performance. A more detailed treatment is presented in [Khatib and Burdick 1985].

8. Problem Formulation

Let $\underline{\Gamma}_{0_i}$ and $\overline{\Gamma}_{0_i}$ be respectively the minimal and maximal bounds of the i^{th} actuator force Γ_i at zero joint velocity. In a configuration $\mathbf{q}$, the minimal value of the amplitude of the i^{th} joint force that is available to contribute to the end-effector acceleration at zero joint velocity is given by

$$\gamma_{0_i}(\mathbf{q}) = \min(|\underline{\Gamma}_{0_i} - g_i(\mathbf{q})|, |\overline{\Gamma}_{0_i} - g_i(\mathbf{q})|). \quad (40)$$

Define the $n \times n$ joint force normalization matrix, $N_0(\mathbf{q})$:

$$N_0(\mathbf{q}) = diag(\gamma_{0_i}(\mathbf{q})); \quad (41)$$

so that the vector of normalized joint forces that are available for the end-effector acceleration is confined to the unit hypercube $\mathcal{D}_f$:

$$\mathcal{D}_f = N_0^{-1}(\mathbf{q}) \prod_{i=1}^{n} [-\gamma_{0_i}(\mathbf{q}), \gamma_{0_i}(\mathbf{q})]. \quad (42)$$

Define the $m_0 \times m_0$ acceleration weighting matrix W:

$$W = \begin{pmatrix} I_{m_p} & 0 \\ 0 & wI_{m_r} \end{pmatrix}; \quad (43)$$

where I_{m_p}, I_{m_r}, and 0 are the identity and zero matrices with the dimensions of the end-effector position and orientation subspaces, m_p and m_r. w is a metric homogeneity weighting coefficient between the linear and angular accelerations of the end-effector. The minimum available weighted acceleration $W\ddot{\mathbf{x}}$ at zero joint velocities is then within the hyperparallelepiped $\mathcal{D}_{a0}$:

$$\mathcal{D}_{a0} = E_0(\mathbf{q})\mathcal{D}_f; \quad (44)$$

where

$$E_0(\mathbf{q}) = WE(\mathbf{q})N_0(\mathbf{q}). \quad (45)$$

The matrix $E_0(\mathbf{q})$ describes the mapping, at zero joint velocities, of the unit hypercube of normalized joint forces (42) into the hyperparallelepiped of weighted accelerations (44). Coriolis and centrifugal forces which arise at non-zero joint velocities modify the values of minimum available joint forces. In addition, at high velocities the actuator force bounds are modified in typical actuators. Let $\overline{\dot{\mathbf{q}}}$ be the vector of maximum operating joint velocities, and let us designate by $\underline{\Gamma}_{v_i}$ and $\overline{\Gamma}_{v_i}$ the lower and upper bounds of the i^{th} actuator force Γ_i at these velocities. The minimal value of the amplitude of the i^{th} joint force that is available to contribute to the end-effector acceleration at $\overline{\dot{\mathbf{q}}}$ becomes

$$\gamma_{v_i}(\mathbf{q}) = \min(|\underline{\sigma}_i(\mathbf{q}) - sign(\underline{\sigma}_i)\nu_i(\mathbf{q})|, |\overline{\sigma}_i(\mathbf{q}) - sign(\overline{\sigma}_i)\nu_i(\mathbf{q})|) \quad (46)$$

where $\underline{\sigma}_i$, $\overline{\sigma}_i$, and ν_i are the i^{th} components of the vectors

$$\begin{aligned} \underline{\sigma}(\mathbf{q}) &= \underline{\Gamma}_v - \mathbf{g}(\mathbf{q}) - \tilde{C}(\mathbf{q})[\overline{\dot{\mathbf{q}}}^2]; \\ \overline{\sigma}(\mathbf{q}) &= \overline{\Gamma}_v - \mathbf{g}(\mathbf{q}) - \tilde{C}(\mathbf{q})[\overline{\dot{\mathbf{q}}}^2]; \\ \nu(\mathbf{q}) &= \mathcal{A}(\tilde{B}(\mathbf{q}))[\overline{\dot{\mathbf{q}}}\,\overline{\dot{\mathbf{q}}}]. \end{aligned} \quad (47)$$

The operator $\mathcal{A}$ produces the matrix of the absolute values of the elements of $\tilde{B}(\mathbf{q})$. $\nu_i(\mathbf{q})$ therefore represents the largest absolute values of Coriolis force that can occur at the i^{th} joint during any motion within the limits of maximum operating joint velocities. At these velocities, the joint force normalization matrix and the hyperparallelepiped of minimum available weighted end-effector acceleration become

$$\begin{aligned} N_v(\mathbf{q}) &= diag(\gamma_{v_i}(\mathbf{q})); \\ \mathcal{D}_{av} &= E_v(\mathbf{q})\mathcal{D}_f; \end{aligned} \quad (48)$$

where

$$E_v(\mathbf{q}) = WE(\mathbf{q})N_v(\mathbf{q}). \quad (49)$$

9. Dynamic Optimization

In manipulator design, dynamic optimization is aimed at providing the largest and the most isotropic and uniform bounds on the end-effector acceleration, or equivalently, on the command vector $\mathbf{F}^*_m$ (36), at both low and high velocities. The $E_0(\mathbf{q})$ and $E_v(\mathbf{q})$ matrices establish the input/output relationships between the normalized minimum available joint forces and the end-effector weighted accelerations at zero and maximum joint velocities. In a given configuration $\mathbf{q}$, the $E_0(\mathbf{q})$ and $E_v(\mathbf{q})$ matrices are expressed as a function of the manipulator's kinematic, dynamic, and actuator parameters; *e.g.* link lengths, masses, inertias, centers of mass, actuator masses, and their force and velocity limits. Let η designate the set of these parameters.

In the manipulator design process, workspace and kinematic considerations will be used first to determine the set of possible kinematic configurations of the mechanism. Kinematic specifications, in addition to dynamic and structure requirements, establish various constraints on some or all of the manipulator design parameters η. Let $\{u_i(\eta); i = 1, \ldots, n_u\}$ and $\{v_i(\eta); i = 1, \ldots, n_v\}$ designate the sets of equality and inequality constraints on the manipulator design parameters η.

The optimization problem can then be formalized in terms of finding the design parameters η, under the constraints $\{u_i(\eta)\}$ and $\{v_i(\eta)\}$, that maximize the volume of the hyperparallelepipeds $\mathcal{D}_{a0}, \mathcal{D}_{av}$ and minimize the ratio of their largest and smallest axes. Expressed as a function of the manipulator configuration q and the design parameters η, the matrices $E_0(\mathbf{q}, \eta)$ and $E_v(\mathbf{q}, \eta)$ are asymmetric. A matrix M can be represented as the product of an orthogonal matrix with the symmetric positive semi-definite matrix $\sqrt{(MM^T)}$, *i.e. the polar decomposition.* While the orthogonal matrix in this decomposition describes the rotation properties of vectors under the mapping by M, $\sqrt{(MM^T)}$ contains the norm or elongation characteristics of these mapped vectors. The largest eigenvalue of $\sqrt{(MM^T)}$ represents, in fact, the Euclidean norm $\|M\|$ of M. In addition, the ratio of this eigenvalue to the smallest one, *i.e.* the *condition number* $\kappa(M)$, characterizes the uniformity of the mapping by M. The condition number has been used to evaluate the kinematic characteristics in articulated hand design [Salisbury and Craig 1982].

Finally, the problem of dynamic optimization over the manipulator work space $\mathcal{D}_\mathbf{q}$ can be expressed as

$$\begin{cases} \min \tilde{\mathcal{C}}(\eta) = \int_{\mathcal{D}} \mathcal{C}(\mathbf{q}, \eta) w(\mathbf{q}) d\mathbf{q} \\ with \begin{cases} u_i(\eta) = 0 & i = 1, \ldots, n_u; \\ v_i(\eta) \leq 0 & i = 1, \ldots, n_v; \end{cases} \end{cases} \tag{50}$$

where the function $w(\mathbf{q})$ is used to relax the weighting of the cost function $\mathcal{C}(\mathbf{q}, \eta)$ in the vicinity of the work space boundaries and singularities. This cost function is given by:

$$\mathcal{C}(\mathbf{q}, \eta) = \frac{1}{\|E_0(\mathbf{q}, \eta)\|} + \alpha_0 \kappa(E_0(\mathbf{q}, \eta))$$
$$+ w_v[\frac{1}{\|E_v(\mathbf{q}, \eta)\|} + \alpha_v \kappa(E_v(\mathbf{q}, \eta))]; \tag{51}$$

where α_0 (*resp.* α_v) is the desired relative weighting between the end-effector acceleration characteristics of isotropicity and magnitude at zero velocity (*resp.* maximum operating velocity). w_v controls the relative importance given to dynamic performance at high velocity.

The optimization of manipulator performance for tasks involving applied end-effector forces can be similarly formulated, using the relation (35). In addition, the optimization of end-effector velocity performance can also be formulated using the manipulator kinematic model and the actuator velocity characteristics. In the manipulator design process, dynamic, kinematic, and applied force characteristics of the end-effector can be incorporated into a global optimization by extending the previous cost function.

10. Application

In the following example, a simple two-link arm has been used [Khatib and Burdick 1985] to illustrate this formulation for the dynamic optimization of manipulator systems. Both joints are assumed to be revolute and to have parallel axes of rotation. l_i, m_i, $\mathbf{r}_i$, and I_i are the length, mass, distance vector from the joint to the center of mass, and the inertia at the center of mass for the i^{th} link. Gravity acts in the plane perpendicular to these axes.

The link lengths are constrained to maintain a maximum extension of l_{max}, and l_i is in $[\underline{l}, \bar{l}]$. Each link is constructed as a solid cylinder, and actuators are located at the joints. The minimum value of the link cylinder radius is expressed as a function of the maximum loading force f_{max}, the structural stress ς, the length, and the material properties of the link. Consequently, link masses and inertias are similarly constrained. Actuators are assumed to have symmetrical peak torques. Their masses and inertias, m_{a_i} and I_{a_i}, are considered to be linearly proportional to the peak torque magnitude. In addition, the joint torques $\underline{\Gamma}_{v_i}$ and $\overline{\Gamma}_{v_i}$ at maximum operating joint velocities (2.0 rad/sec) are reduced to 70% of their values at zero velocity ($\underline{\Gamma}_{0_i}$, $\overline{\Gamma}_{0_i}$). The set η of design parameters consists of $\{l_i, m_i, I_i, r_{x_i}, m_{a_i}, I_{a_i}, \underline{\Gamma}_{0_i}, \overline{\Gamma}_{0_i}\}$. The end-effector equations of motion and the sets of equality and inequality constraints, $u_i(\eta)$ and $v_i(\eta)$, associated with this mechanism are given in [Khatib and Burdick 1985].

Figures (2) and (3) illustrate the dynamic performance for two different arm designs. The parallelepipeds in the upper left figures (a) depict the boundaries on minimum available end-effector acceleration at zero joint velocities. The largest circles that can be inscribed within these boundaries, which represent the magnitude of available isotropic accelerations, are shown in the upper right figures (b). The lower figures (c,d) illustrate these accelerations at maximum operating joint velocities. Let $\overline{a}_0$ and $\overline{a}_v$ be the average magnitude of available isotropic acceleration over the workspace at zero and maximum joint operating velocities, respectively.

The dynamic performance shown in Figure 2 corresponds to an initial set of design parameters. These parameters are based on kinematic, joint inertia, and gravity loading considerations; and the mass and inertia parameters are at their minimums. However, this design yields poor isotropic end-effector acceleration characteristics. In addition, the magnitude of the minimum available acceleration at maximum operating velocity is appreciably reduced. $\overline{a}_0$ and $\overline{a}_v$ are $38.3m/sec^2$ and $19.0m/sec^2$, respectively.

Figure 3 shows the results of an optimization of the above arm with the given constraints. At zero velocity, $\overline{a}_0$ is $59.7m/sec^2$, which represents an improvement of 56% over the initial design. More significantly, at maximum velocity $\overline{a}_v$ is $35.1m/sec^2$, an increase of 85% relative to the initial arm. In this improved design, the actuator torques required are only 6.0% higher than those used in the initial design.

11. Conclusion

We have presented the operational space formulation and the unified approach to motion and active force control of manipulator systems. A two-level control architecture has been designed to increase the system's real-time performance. We have also presented the extension of this formulation to redundant manipulator mechanisms, and have discussed the basic methodology of dealing with kinematic singularity problems. Results of the preliminary implementation in COSMOS have shown the operational space formulation to be an effective means of achieving high dynamic performance in real-time motion control and active force control of robot manipulators for more advanced assembly tasks. In the design of manipulator systems, the dynamic optimization problem has been formal-

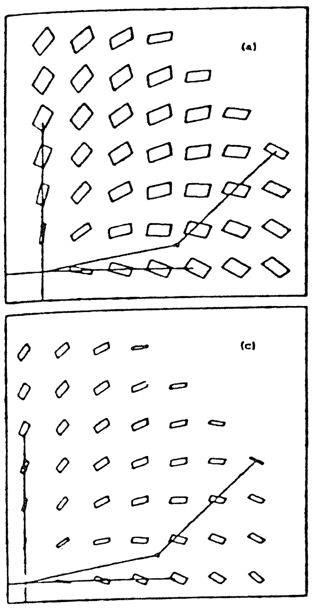

$l_1 = 0.5m,\ m_1 = 12.5kg,\ r_{x1} = 0.25m,\ r_{y1} = 0,\ I_1 = 1.602kg.m^2;$
$l_2 = 0.5m,\ m_2 = 9.5kg,\ r_{x2} = 0.25m,\ r_{y2} = 0,\ I_2 = 0.664kg.m^2;$
$\overline{\Gamma}_{01} = 500Nm,\ \overline{\Gamma}_{v1} = 350Nm,\ \overline{\Gamma}_{02} = 200Nm,\ \overline{\Gamma}_{v2} = 140Nm.$

Figure 2. Initial Design

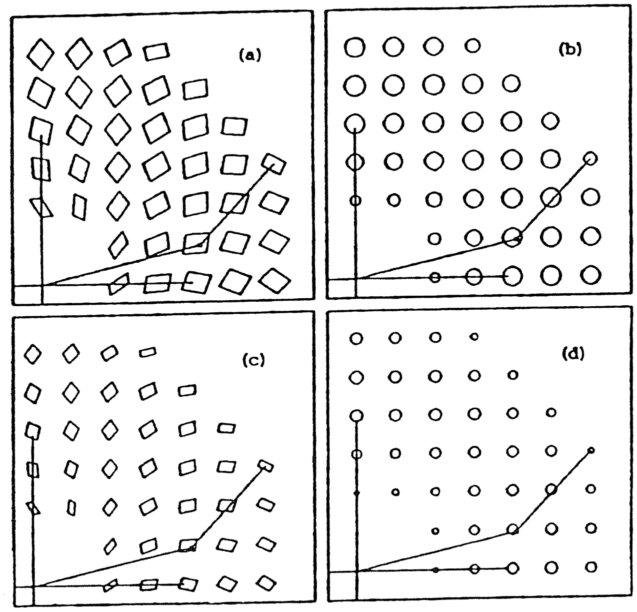

$l_1 = 0.60m,\ m_1 = 16.92kg,\ r_{x1} = 0.20m, r_{y1} = 0,\ I_1 = 1.93kg.m^2;$
$l_2 = 0.4m,\ m_2 = 6.09kg,\ r_x2 = 0.21m,\ r_{y2} = 0,\ I_2 = 0.39kg.m^2;$
$\overline{\Gamma}_{01} = 612Nm,\ \overline{\Gamma}_{v1} = 428Nm,\ \overline{\Gamma}_{02} = 130Nm,\ \overline{\Gamma}_{v2} = 91Nm.$

Figure 3. Optimized Design

ized using the end-effector equations of motion in operational space. The characteristics of the relationship that governs the transfer of joint forces to end-effector accelerations have been used for the evaluation of manipulator dynamic performance. The optimization problem has been expressed as the minimization, with respect to the design parameters and constraints, of a cost function based on these characteristics.

The large isotropic and uniform bounds on end-effector acceleration provided by this dynamic optimization will be translated into a large and well conditioned operational space command vector. This will provide the control system, in addition to the forces necessary for end-effector dynamic decoupling, sufficient operational forces to achieve the desired design performance throughout the workspace. The kinematic characterization and optimization of manipulators can be similarly formulated. A global optimization integrating kinematic and dynamic criteria can be achieved.

References

Asada, H. 1983 (September). A Geometrical Representation of Manipulator Dynamics and Its Application to Arm Design. Trans. of ASME, Journal of Dynamic Systems, Measurement, and Control, Vol. 105, No. 3, pp. 131-135.

Asada, H. and Cro Granito, J. A. 1985 (March 25-28). Kinematic and Static Characterization of Wrist Joints and Their Optimal Design. Proceedings of the 1985 International Conference on Robotics and Automation, pp. 244-250, St. Louis.

Craig, J.J. and Raibert, M. 1979. A Systematic Method for Hybrid Position/Force Control of a Manipulator. Proceedings 1979 IEEE Computer Software Applications Conference, Chicago.

Fournier, A. 1980 (April). Génération de Mouvements en Robotique. Application des Inverses Généralisées et des Pseudo-Inverses. *Thèse d'Etat*, Mention Science, Université des Sciences et Techniques des Languedoc, Montpellier, France.

Hanafusa, H., Yoshikawa, T., and Nakamura, Y., 1981. Analysis and Control of Articulated Robot Arms with Redundancy. 8th IFAC World Congress, Vol. XIV, pp. 38-83.

Hewit, J.R. and Padovan, J. 1978 (September). Decoupled Feedback Control of a Robot and Manipulator Arms. Proceedings Third CISM-IFToMM Symposium on Theory and Practice of Robots and Manipulators, 251-266, Udine, Italy (Elsevier 1979).

Hollerbach, J.M. 1984 (August). Optimum Kinematic Design for a Seven Degree of Freedom Manipulator. Prep. of the 2nd International Symposium of Robotics Research, pp. 349-356, Kyoto, Japan.

Hollerbach, J.M. and Suh, K.C. 1985 (March 25-28). Redundancy Resolution of Manipulators Through Torque Optimization. 1985 International Conference on Robotics and Automation. St. Louis.

Khatib, O. Llibre, M. and Mampey, R. 1978 (July). Fonction Décision-Commande d'un Robot Manipulateur. Rapport Scientifique no. 2/7156 RA, DERA-CERT, Toulouse, France.

Khatib, O. and Le Maitre, J.F. 1978 (September 12-15). Dynamic Control of Manipulators Operating in a Complex Environment. Proceedings Third CISM-IFToMM Symposium on Theory and Practice of Robots and Manipulators, 267-282, Udine, Italy (Elsevier 1979).

Khatib, O. 1980 (December). Commande Dynamique dans l'Espace Opérationnel des Robots Manipulateurs en Présence d'Obstacles. Thése de Docteur-Ingénieur. École Nationale Supérieure de l'Aéronautique et de l'Espace, Toulouse, France.

Khatib, O. 1983 (December 15-20). Dynamic Control of Manipulators in Operational Space. Sixth CISM-IFToMM Congress on Theory of Machines and Mechanisms, pp. 1128-1131, New Delhi, India (Wiley, New Delhi).

Khatib, O. 1985 (March 25-28). Real-Time Obstacle Avoidance for Manipulators and Mobile Robots. Proceedings of the 1985 International Conference on Robotics and Automation, pp. 500-505, St. Louis.

Khatib, O. Burdick, J. and Armstrong, B. 1985. Robotics in Three Acts - Part II (Film). Artificial Intelligence Laboratory, Stanford University.

Khatib, O. and Burdick, J. 1985 (November). Dynamic Optimization in Manipulator Design: The Operational Space Formulation. The 1985 ASME Winter Annual Meeting, Miami.

Khatib, O. and Burdick, J. 1986 (April). Manipulator Motion and Force Control. The 1986 International Conference on Robotic and Automation, San Francisco.

Liegois, A. 1977 (December). Automatic Supervisory Control of the Configuration and Behavior of Multibody Mechanisms. IEEE Transactions on Systems, Man and Cybernetics, Vol. 7, No. 12.

Luh, J.Y.S. Walker, M.W. and Paul, P. 1980 (June). Resolved Acceleration Control of Mechanical Manipulators. IEEE Transactions on Automatic Control, no. 3, pp. 468-474.

Luh, J.Y.S. and Gu, Y.L. 1985 (March). Industrial Robots with Seven Joints. Proc. 1985 IEEE International Conference on Robotics and Automation, pp. 1010-1015, St. Louis.

Mingori, D.L. 1970. A Stability Theorem for Mechanical Systems with Constraint Damping. Journal of Applied Mechanics, Transactions of the ASME, pp. 253-258.

Paul, R.P. and Shimano, B. 1976 (July). Compliance and Control. Proceedings of the Joint Automatic Control Conference. pp. 694-699. Purdue University.

Paul, R.P and Stevenson, C.N. 1983. Kinematics of Robot Wrists. International Journal of Robotics Research, Vol. 2, No. 1, pp. 31-38.

Renaud, M. 1975 (December). Contribution à l'Etude de la Modélisation et de la Commande des Systèmes Mécaniques Articulés. Thèse de Docteur Ingénieur. Université de Paul Sabatier, Toulouse.

Renaud, M. and Zabala-Iturralde, J. 1979 (Mars). Robot Manipulator Control. Proceeding of the 9th International Symposium on Industrial Robots. pp. 463-475, Washington, D.C.

Roth, B. 1976. Performance Evaluation of Manipulators from a Kinematic Viewpoint. National Bureau of Standards Workshop on Performance Evaluation on Programmable Robots and Manipulators, National Bureau of Standards, NBS SP-459, pp. 39-61.

Rumiantsev, V.V. 1970. On the Optimal Stabilization of Controlled Systems. PMM, Vol. 34, No. 3, pp. 440-456.

Salisbury, J.K. 1980 (December) Active Stiffness Control of a Manipulator in Cartesian Coordinates. 19th IEEE Conference on Decision and Control, Albuquerque, New Mexico.

Salisbury, J.K. and Craig, J.J. 1982. Articulated Hands: Kinematic and Force Control Issues. International Journal of Robotics Research, Vol. 1,No. 1, pp. 4-17.

Shimano, B. 1978 (March). The Kinematic Design and Force Control of Computer Controlled Manipulators. Stanford A.I. Lab. Memo 313.

Takase, K. 1977. Task-Oriented Variable Control of Manipulator and Its Software Servoing System. Proceedings of the IFAC International Symposium, pp. 139-145, Tokyo.

Whitney, D.E. 1969 (June). Resolved Motion Rate Control of Manipulators and Human Prostheses IEEE Transactions on Man Machine Systems, No. 10, Vol. 2, pp. 47-53.

Whitney, D.E. 1977 (June). Force Feedback Control of Manipulator Fine Motions. ASME, Journal of Dynamic Systems, Measurement, and Control, pp. 91-97.

Whitney, D.E. 1985 (March). Historical Perspective and State of the Art in Robot Force Control. Proceedings of the 1985 IEEE International Conference on Robotics and Automation, pp. 262-268, St. Louis.

Yoshikawa, T. 1983. Analysis and Control of Robot Manipulators with Redundancy. Proc. of the 1st International Symposium of Robotics Research, MIT Press, Cambridge, MA, pp. 735-747.

Yoshikawa, T. 1985 (March). Dynamic Manipulability of Robot Manipulators. Proc. 1985 IEEE International Conference on Robotics and Automation, St. Louis, pp. 1033-1038.